AALBORG UNIVERSITY

Centralized and Distributed Solutions for Fast Muting Adaptation in LTE-Advanced HetNets

Soret, Beatriz; Pedersen, Klaus I.

Centralized and Distributed Solutions for Fast Muting Adaptation in LTE-Advanced HetNets

Beatriz Soret, *Member IEEE,* and Klaus I. Pedersen, *Member IEEE*

Abstract—Enhanced Intercell Interference Coordination (eICIC) is known to provide promising performance benefits for LTE-Advanced Heterogeneous Networks. The use of eICIC facilitates more flexible inter-layer load balancing by means of small cell Range Extension (RE) and Almost Blank Subframes (ABS). Even though the eICIC configuration (RE and ABS) ideally should be instantaneously adapted to follow the fluctuations of the traffic and the channel conditions over time, previous studies have focused on slow intercell coordination. In this paper, we investigate fast dynamic eICIC solutions for centralized and distributed Radio Resource Management (RRM) architectures. The centralized RRM architecture assumes macro and Remote Radio Heads (RRHs) inter-connected via high-speed fronthaul connections, while the distributed architecture is based on traditional macro and pico cells deployments with X2 backhaul interface. Two different fast muting adaptation algorithms are derived, and it is shown how those can be appplied to both the centralized and the distributed architecture. Performance results with bursty traffic show that the fast dynamic adaptation provides significant gains, both in 5%-ile and 50%-ile user throughput, as well as improvements in user fairness. The best performance is naturally obtained for the centralized architecture, although the performance of the distributed architecture is comparable for the cases where enhanced X2 intercell information exchange is exploited.

Index Terms—Heterogeneous Networks, eICIC, Almost Blank Subframes, muting adaptation, LTE-Advanced.

I. INTRODUCTION

Migration from macro-only networks to heterogeneous networks (HetNet) is a promising method for increasing the capacity of cellular systems such as LTE-Advanced networks [1]. A HetNet consists of a mixture of macro cells and smaller low power nodes such as pico and femto cells. Various aspects of cellular HetNets have been extensively studied in academia, industry, and standardization bodies such as 3GPP [2]. In this study we focus on the downlink performance of LTE-Advanced co-channel HetNet deployments [2] [3], meaning that macro and small cells are using the same carrier frequency. One of the main challenges in this scenario is the macro interference to the users in the small cells [4], which can be alleviated by the use of enhanced intercell interference coordination (eICIC) [5] [6]. Here, the macro base station (called eNB in LTE) plays the role of the aggressor, whereas small cell UEs in the cell-edge are the victims.

A. Scope and Related Work

In co-channel deployments, the small cell range can be extended to offload more macro users to the low power nodes. By doing so, the experienced interference level by the users served at the small cell layer increases. The eICIC scheme relies on time-domain interference coordination between the macro and the small cell layer, where some subframes are partially muted at the macro layer to lower the interference to the small cell users. eICIC is a natural enabler of traffic load balancing between different cell types, yielding better overall system level performance and a higher end-user throughput. Therefore, the load balancing optimization and the eICIC muting pattern are intimately related. Many studies in the literature have addressed the cell association optimization problem and related load balancing methods, often identified as one of the essential Self-Organizing Networks (SON) features [7] [8]. For example, in [9] the authors propose a load-aware user association scheme that is evaluated in fully loaded networks. In [10] the authors investigate the optimal muting adaptation for a given number of victim users. In [11] the challenge of the optimal eICIC muting and the load balancing is addressed by formulating a joint optimization problem, assuming the same muting ratio for all the macro cells and constant spectral efficiencies (slow-time-scale adaptation).

Ideally, the eICIC muting pattern should be instantaneously adapted to follow the time-variant load fluctuations. However, most of the studies in the open literature [5] - [6], [10] - [16] have focused on slow inter-cell coordination and, consequently, slow muting adaptation. This implies that muting patterns cannot track fast traffic fluctuations, but rather aim at capturing the envelope of the average traffic variations. In this paper we propose an eICIC framework for performing fast muting adaptation independently at each macro cell. We narrow the scope of the paper to the problem of fast muting adaptation, motivated by the lack of public research findings in this direction, assuming that the load balancing is optimized in parallel by means of existing algorithms from the literature.

The majority of the published eICIC studies have focused on cases where the small cells are realized with pico cells [5] - [16] or closed subscriber group femto cells [17]. For the cases with macro and pico, it is typically assumed that each cell has its own radio resource management (RRM) algorithms including packet scheduling, link adaptation and hybrid ARQ [18], while the coordination of the eICIC muting patterns is supported via the backhaul X2 interface between the different eNBs. Due to the X2 signaling delays, and for the sake of the overall system stability, it is typically assumed that muting patterns are only updated on a slow time scale of several

B. Soret and K. I. Pedersen are with Nokia Solutions and Networks, Denmark (e-mail: beatriz.soret@nsn.com, klaus.pedersen@nsn.com). K. I. Pedersen is also with Aalborg University.

seconds [16].

An alternative implementation consists of deploying Remote Radio Heads (RRH) instead of pico cells. Each RRH is connected via a high-speed low latency fronthaul to a macro cell, enabling centralization of the major RRM algorithms in the macro eNB. This essentially means that the architecture offers further opportunities for intercell RRM algorithms in clusters of connected macro and RRHs, like e.g. fast decisions on whether a subframe shall be muted or not.

B. Overview of the paper

The main contributions of this paper are:

- An extended version of the eICIC framework for fast muting decisions in [19] is presented, based on enhanced subframe classification and proper measurement report configuration of the small cell users.
- Two different dynamic algorithms for the fast muting adaptation are proposed. The first one, based on instantaneous load of the two layers, requires only the information of the number of users in the macro and the small cell layer. The second algorithm, based on average Proportional Fair (PF) metrics, aims at balancing the PF metrics between layers.
- The fast muting adaptation algorithms are tailored to be applied in centralized RRM architectures with macro and RRHs, where all the necessary information is available at the macro. Nevertheless, we show that the algorithms can also be decomposed to be applicable in distributed architectures based on X2 information exchange. Needless to say, the rate of adaptation limits the eICIC gain in these cases. It is investigated how to best operate the distributed RRM solutions to achieve a performance close to the centralized RRM solution.

Our priority is to study the performance of the derived schemes under realistic conditions, including the effect of major RRM algorithms under time-variant bursty traffic conditions. In order to achieve this target, we use state-of-the-art system level simulation methodologies to obtain statistical reliable results with a high degree of accuracy.

The rest of the paper is organized as follows. Section II introduces the network and the traffic model, as well as the different intercell RRM solutions under study.

In Section III the eICIC framework is presented.

Section IV describes the two proposed fast muting adaptation algorithms, and it is discussed how to operate them in centralized and distributed architectures. In Section V we analyze the performance of the two proposed algorithm with ideal and non-ideal conditions, and with different degrees of intercell coordination. Finally, concluding remarks are given in Section VI.

II. SETTING THE SCENE

A. Network Model

The baseline eICIC network model is illustrated in Figure 1. We assume an LTE-Advanced network with macro cells and small cells. A cluster is composed by
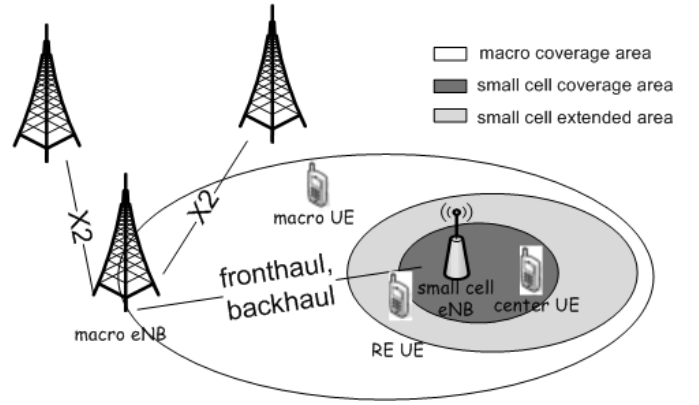

Fig. 1. System Model.

one macro cell and a set of small cells in its coverage area, $\mathcal{C} = \{C^m, C^1, ..., C^s, ...C^S\}$, with $1 \leq s \leq S$ and $\{s, S\} \in \mathbb{N}$. Both the UEs and the eNBs are equipped with two antennas. The macro eNBs are inter-connected through X2 interface. The connection between the macro and the small cells can be backhaul or fronthaul, as it will be further explained in Section II-C.

We use commonly accepted random deployment models for small cells and UEs [20]. In brief, three-sector macro eNBs are placed in a regular hexagonal grid, assuming 46 dBm transmit power per antenna. A constant number of small cells with 30 dBm per antenna are placed randomly in each macro cell area according to a spatial uniform point process, subject to minimum distance constraints between different cell types as defined in [21].

The macro and the small cells share the same bandwidth (co-channel deployment), and UEs are only connected to one eNB at a time. In order to select the best serving cell, UEs measure the reference signals of nearby cells. However, the large difference in downlink transmit power among macro and small cell eNBs significantly reduces the coverage area of the small cells, and UEs will tend to connect to high-power macro cells rather than to low-power small cells. This imbalance is compensated by expanding the range of the small cell. A positive bias denoted as Range Extension (RE) offset is added to the Reference Signal Received power (RSRP) measured from small cell eNBs, pushing more UEs to this layer [6]. Therefore, the criterion to select the serving cell is given by:

$$\underset{j \in \mathcal{C}}{\arg \max} \{RSRP_j + RE_j\} \quad (1)$$

where the terms in (1) are expressed in dB, $RSRP_j$ is the RSRP measured from eNB j and RE_j is the offset applied to eNB j. $RE_j = 0$ dB for all macro eNBs, while typical values for small cell RE offsets are 3, 6, 9, and 12 dB. The value of the RE offset, which is signaled to the UEs using the Radio Resource Control (RRC) protocol, is adjusted based on SON-based load-balancing algorithms on a relative slow time-scale, in order to avoid excessive RRC signaling overhead at the air-interface [7].

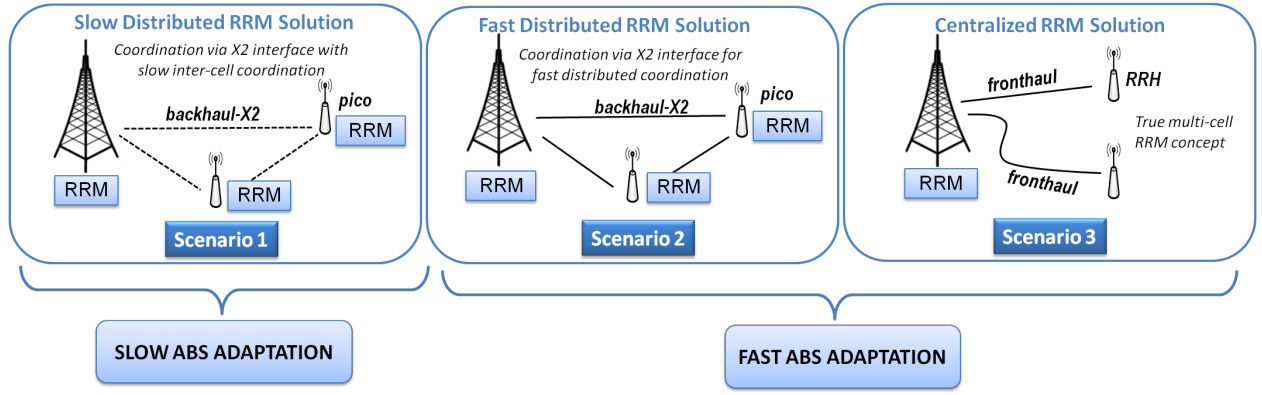The RE offset balances the network load at the cost of poorer

Fig. 2.   RRM Architectures.

Signal to Interference and Noise Ratio (SINR) for the small cell users, which suffer from strong macro interference and lower signal strength from their serving eNB. One solution to cope with this problem is to prevent macro eNBs from transmitting on certain subframes. During the muted subframes, the macro cell still transmits essential system information and Common Reference Signals (CRS) in order to provide support to the legacy UEs. The muted (or protected) subframes are therefore named Almost Blank Subframes (ABS) [16]. Macro users are not scheduled during those subframes, leading to lower macro interference. It is therefore possible for the small cells to serve UEs that are located in the extended area outside the default small cell coverage, enabling the application of higher values of RE. We define β to be the muting ratio, with $0 \le \beta \le 1$. For example, $\beta = 0.5$ means that the macro cell schedules users only in half of the subframes.

B. Traffic Model

The traffic model plays an important role in analyzing the performance of HetNets [13] [22]. We assume a dynamic traffic model with Poisson call arrival and finite payload size per call B. Once the payload has been successfully delivered to the UE, the call is terminated. We define both the total arrival rate λ per cluster (i.e. macro cell area) and the average offered traffic load $\bar{L} = \lambda \cdot B$ per cluster. If the payload is small, the users transmit their load very fast, leading to significant traffic fluctuations in the system. It is crucial in this case to rapidly adapt to these fluctuations. On the other hand, with large values of B the traffic variations will be slower, and the benefits of having fast muting adaptation will be less remarkable. The finite buffer model has been adopted to model FTP traffic [23]. eculiarities explained next.

C. RRM Architectures

The three RRM architectures in Figure 2 are analyzed:

1) Slow Distributed RRM Solution: The majority of existing eICIC studies have focused on Scenario 1 in Figure 2, where a number of small cells in the form of pico cells are deployed in the macro coverage area. Each cell has its own RRM

functionality. 3GPP Rel. 10 provides the mechanisms to co-ordinate and exchange information of the eICIC configuration (β and RE) between eNBs [5], which is typically updated on a slow time scale of several seconds (semi-statically configured). Scenario 1 is used as the baseline reference, and it will be shown that a tighter intercell coordination can increase the performance of the network.

2) Fast Distributed RRM Solution: Scenario 2 has the same distributed RRM architecture as for Scenario 1, but instead of slow or semi-static adaptation, β is dynamically adjusted by exploiting enhanced information exchange over X2. For the sake of simplicity, no explicit coordination is enforced between neighboring clusters, so the intercell fast adaptation is conducted only at a cluster level.

3) Centralized RRM Solution: In Scenario 3 the small cells are deployed in the form of RRHs, connected to the macro eNB through a low latency, high bandwidth link (fronthaul). All RRM algorithms for both the macro and small cells belonging to the same cluster are implemented in the macro eNB. Obviously, the centralized approach opens a wide range of opportunities to improve the overall HetNet performance e.g. via joint multi-cell RRM decision making.

D. Performance Metrics

The main Key Performance Indicator (KPI) that we aim at maximizing in this study is related to the downlink experienced end-user throughput. In particular, we focus on maximizing the 5%-ile outage user throughput of the system, but also statistics of the 50%-ile (median) user throughput are monitored and presented. The system capacity per cluster is defined as the maximum offered throughput that can be tolerated for a certain minimum 5%-ile outage user throughput, and it is used for comparing the relative capacity gains of the fast muting adaptation algorithms as compared to the case with slow adaptation. Finally, we also aim at comparing the user fairness of the different schemes through the Jain's fairness index [24]:

$$J(R_1; R_2; ...; R_U) = \frac{(\sum_{u=1}^{U} R_u)^2}{U \sum_{u=1}^{U} R_u^2} \qquad (2)$$
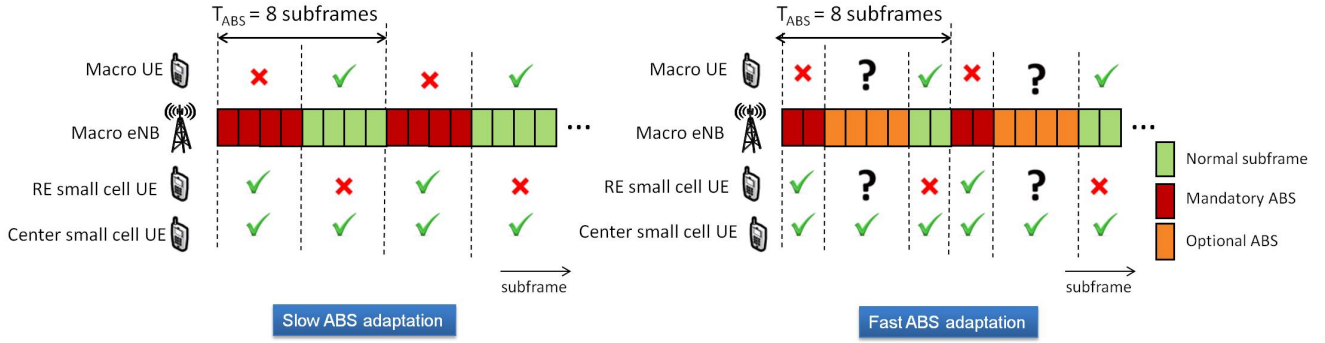
Fig. 3. Subframe classification at the macro layer for slow and fast ABS adaptation.

where R_u is the throughput of user u and U is the total number of users. The index reaches the maximum of one when all users experience the same throughput.

Given these KPIs, our study objective is to derive simple and robust fast muting adaptation algorithms that provide promising capacity gains without jeopardizing the user fairness, as compared to what is achievable with known slow muting adaptation schemes.

III. eICIC FRAMEWORK

A. Subframe Classification

1) Slow Muting Adaptation: The slow or semi-static ABS adaptation (Scenario 1) involves two kinds of subframes, as shown in Figure 3: Normal subframes and mandatory ABS, with a periodically repeated muting pattern. As shown in Figure 3, macro users are only scheduled during normal subframes. The small cell center users are not affected so much by macro interference, whereas RE users suffer from strong inter-layer interference during normal subframes. Therefore, resource allocation should aim at protecting RE users by allocating them during subframes overlapping mandatory ABS, when the macro interference is minimized. Only if those subframes cannot be filled by the UEs in the extended area, the centre UEs might compete for the remaining resources.

2) Fast Muting Adaptation: To enable fast muting decisions (Scenarios 2 and 3), the muting ratio shall be adjusted on a subframe basis. For this purpose we define a new kind of subframe in the macro layer (see Figure 3), named optional ABS. Shortly before the begining of an optional ABS, the macro cell decides if it should be used as *normal* or *ABS*. It is worth mentioning that the notation *optional ABS* is just internal eNB notation, and not known by the UEs. Analogously to the slow case, the pattern of normal, mandatory and optional ABS is synchronized among eNBs. During ABS (mandatory ABS and optional ABS used as ABS) the scheduler should aim at allocating RE users, and schedule center users only if some reaming resources are still available after the allocation of the RE users. If the number of optional ABS per period is low, then most of the resources are semi-statically configured and the adaptation to the traffic fluctuations will be rougher. As the density of optional subframes increases, the dynamicity of the adaptation increases. It is convenient to define at

least one normal and one mandatory ABS subframe for UE measurement and feedback purposes, as discussed next.

B. UE Support

Besides the coordination among eNBs, explicit UE assistance is important for efficient eICIC operation [22]. In LTE, the UE feeds back Channel Quality Indicators (CQIs) to its serving cell to assess radio channel conditions. The CQI is used by the cell to perform accurate link adaptation (i.e. selection of modulation and coding scheme) as well as for packet scheduling purposes. As eICIC involves on/off switching of the macro-cells on a subframe resolution, it naturally causes large interference fluctuations for the small cell UEs. Under these conditions, small cell UEs can be configured by the network to perform time-domain restricted measurements [16]. The basic principle is that small cell UEs are configured to report two separate CQI reports, one corresponding to subframes where the macro uses normal transmission, and one corresponding to subframes where the macro uses ABS. As the configuration of UE measurement restrictions happens via dedicated Radio Resource Control (RRC) signaling [22], it is desirable to have the same measurement configuration for a longer time-period to avoid unnecessary signaling overhead. For eICIC with slow ABS adaptation, this is simply achieved by configuring the UEs to measure separate CQI for subframes set to ABS and normal transmission, as illustrated in Figure 4 (left). For the case with fast ABS adaptation, the UE can be configured to perform CQI measurements only on the subframes that are semi-statically configured as mandatory ABS and normal subframes. It does not perform measurements during optional ABS, as those can switch on a fast basis between ABS and normal transmission. The UE CQI measurement configuration for the case with fast ABS adaptation is illustrated in Figure 4 (right). It is also implied that the small cell decides which CQI (corresponding to ABS or normal) shall be used for link adaptation and packet scheduling decisions for each subframe, depending on whether the macro is using ABS or normal transmission.

When a macro cell transmits ABS, the victim small cell UE is still exposed to macro CRS interference as this is transmitted from the macro in all subframes. Assuming a 2x2 MIMO configuration, the CRS transmission power is
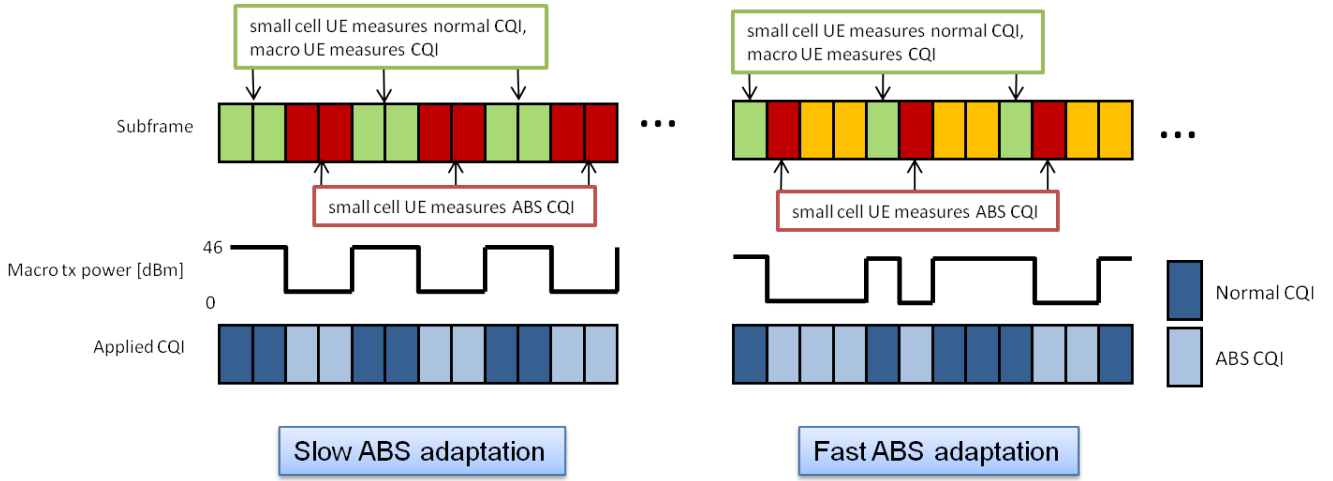
Fig. 4. Measurement report configuration for slow and fast ABS adaptation.

approximately 9% of the total eNB power [25]. As the CRS transmission is a constant deterministic sequence for each cell, it is possible for the UE to estimate the CRS interference from strongly interfering cells, followed by non-linear interference cancellation (IC). To fully benefit from eICIC operation, the 3GPP Rel-11 standard includes a new UE feature to have small cell UEs perform CRS IC from dominant interfering macro cells [22] [26]. This essentially means that small cell UEs with CRS IC ideally experience zero macro interference when ABS is used.

C. Scheduler

The scheduling algorithm assigns the available resources to the corresponding users. In this paper we select a commonly used scheduler, Proportional Fair (PF) [27]. PF is applied separately at each cell (macro cell and each small cell), since users are connected to only one cell. Thus, the resource element at cell C^c at time i is assigned to the user that maximizes the following scheduling metric:

$$\arg \max_u \{M_{u,k}(i)\} \qquad (3)$$

where u is the user index, and k is the Physical Resource Blocks (PRB) group index. According to the LTE physical layer structure, one PRB is the minimum resource element, constituted of 12 consecutive subcarriers with sub-carrier spacing of 15 kHz, for one transmission time interval.

The scheduling metric of PF equals:

$$M_{u,k}(i) = \frac{\hat{r}_{u,k}(i)}{\hat{R}_u(i)} \qquad (4)$$

where $\hat{r}_{u,k}(i)$ is the estimated throughput for user u at the kth PRB group at time i, and $\hat{R}_u(i)$ is the estimated long-term average throughput for that user at time i, that is obtained with an exponential moving average filter. In the case of a small cell user, $\hat{r}_{u,k}(i)$ is based on the CQI reported by the user either on the last normal subframe or on the last mandatory ABS.

In Scenarios 1 and 2 the small cell packet scheduler needs to be dynamically updated with the current ABS configuration in order to apply the suitable CQI for a proper $\hat{r}_{u,k}(i)$ estimation. In Scenario 3 the packet scheduler is centralized in the macro, and thus it is straightforward for the packet scheduler to apply the proper measure during optional ABS depending on whether the subframe is going to be used as ABS or normal.

IV. FAST MUTING ADAPTATION

Two different algorithms are proposed for fast muting adaptation: The first one is based on the instantaneous load at the macro and small cell layer, and the second one is based on the PF metrics.

A. Notation

In our derivation of the algorithms, we distinguish among three kinds of users with very different interference conditions (Figure 1): First of all we have the macro users connected to the macro eNB. Secondly, in the small cell we have center users in the default coverage area of the small cell; and RE users in the extended area of the small cell and connected to it due to the application of the RE offset. Moreover, we define the following notation:

- u_{macro} is the total number of active users connected to the macro cell.
- u_{small} is the total number of active users connected to the small cells within the cluster.
- u_{center} is the total number of active small cell center users connected to small cells within the cluster.
- u_{RE} is the total number of active small cell users in the cell-extended area within the cluster (RE users).
- U is the total number of active users in the cluster: $U = u_{\text{macro}} + u_{\text{small}} = u_{\text{macro}} + u_{\text{center}} + u_{\text{RE}}$.
- $P^c(i)$ is the transmit power of cell C^c at subframe i.
- P^c_{max} is the maximum transmit power of cell C^c, in this study 46 dBm for macro cells and 30 dBm for small cells.

- P_{base}^c is the transmission power of eNB at cell C^c when it is muted.
- $T_{ABS} \in \mathbb{N}$ is the ABS period, 8 in this paper (Figure 3).
- z and n count the number of subframes used as ABS and normal in the current ABS period, respectively. $1 \leq z < T_{ABS}$, $1 \leq n < T_{ABS}$, with $z \in \mathbb{N}, n \in \mathbb{N}$, i.e. at least one subframe is configured as mandatory ABS and another one as normal subframe. The counters are increased everytime a subframe is used as protected or normal resource, respectively, and reset at the beginning of the ABS period. At the end of the ABS period, $\beta = z/T_{ABS}$.
- $sf(i)$ refers to the kind of subframe at time i, with $sf(i) \in \{\text{NORMAL, MANDATORY, OPTIONAL}\}$
- PF^m is the average of the PF metrics of macro users taken during non-ABS.
- PF^s is the average of the PF metrics of small cell users taken only during ABS.

B. Instantaneous Load Based Algorithm (IL-ABS)

The main principle of the Instantaneous Load Based Algorithm (IL-ABS) consists of checking the load at the macro and small cell layer at each optional ABS, and based on those measures it should be decided whether the optional ABS shall be used as normal subframe or protected subframe.

The load in the small cell layer is defined as the percentage of users in the RE area as compared to the total number of users in the cluster, and analogously in the macro layer with the percentage of macro users. Notice that the load measure in the small cell layer refers only to RE users, since those are the ones benefiting more from ABS resources.

The dynamics of the algorithm is as follows: For each optional ABS, the algorithm ensures first of all that the percentage of macro users is served with an appropriate percentage of full power subframes:

$$u_{\text{macro}} \ / \ U \ < \ n \ / \ T_{ABS} \tag{5}$$

If (5) is fulfilled, then it is checked whether the percentage of ABS resources assigned so far is lower than the percentage of high-interfered users:

$$u_{\text{RE}} \ / \ U \ > \ z \ / \ T_{ABS} \tag{6}$$

If (6) is true, the current subframe is muted, and the RE users will have an opportunity to be scheduled in the next subframe. Therefore the algorithm ensures first of all the service of macro users, since the coverage area of the macro eNB is much larger, and the macro cell-edge users do not have the option of being scheduled with reduced interference conditions. The pseudo-code of the algorithm is illustrated in Algorithm 1.

It is worth noting that the application of the algorithm within a cluster may likely lead to the use of different muting patterns in neighbouring macros. Having a tight coordination between macro cells to have exactly the same ABS patterns gives the best performance with slow muting adaptation [12]. However, as it will be shown in the performance results, the gain from dynamically adjusting the ABS is still very significant despite the lack of inter-macro coordination.

Algorithm 1   `Instantaneous Load Based Algorithm (IL-ABS)`

1: $iter = 0$
2: **while** $(iter < iter_{\max})$ **do**
3:    **if** $(iter \bmod T_{ABS} == 0)$ **then**
4:      $n = 0$
5:      $z = 0$
6:    **end if**
7:    **switch** $(sf(iter))$
8:    **case** NORMAL**:**
9:      $P^m(iter) = P_{\max}^m$
10:     $n = n + 1$
11:    **case** MANDATORY**:**
12:     $P^m(iter) = P_{\text{base}}^m$
13:     $z = z + 1$
14:    **default:**
15:     {Optional Subframe}
16:     **if** ($u_{\text{RE}}\ /\ U\ >\ z\ /\ T_{ABS}$) **and** ($u_{\text{macro}}\ /\ U\ <\ n\ /\ T_{ABS}$) **then**
17:      $P^m(iter) = P_{\text{base}}^m$ {Use it as ABS subframe}
18:      $z = z + 1$
19:     **else**
20:      $P^m(iter) = P_{\max}^m$ {Use it as normal subframe}
21:      $n = n + 1$
22:     **end if**
23:    **end switch**
24:    **for** $s = 1 : S$ **do**
25:     $P^s(iter) = P_{\max}^s$ {Pico always at full power}
26:    **end for**
27:    $iter = iter + 1$
28: **end while**

C. Proportional Fair Based Algorithm (PF-ABS)

The second proposal, Proportional Fair Based Algorithm (PF-ABS), is based on the PF metrics at the macro and small cell layer. As shown in (4), the PF metric captures not only the average throughput achieved by the user, but also their instantaneous channel condition. With the average of the PF metrics we have a valuable indicator of the ratio channel condition / average throughput in the cell. The idea is to use the averaged PF metrics in the macro and small cell layer as indicators of whether the layer throughput is improving or deteriorating, i.e. an estimation on whether we should assign more or less resources to the layer.

In the macro layer the average PF metric of all users during normal transmission is calculated as:

$$PF^m(i) = \frac{1}{u_{\text{macro}}} \sum_{u=1}^{u_{\text{macro}}} \sum_{k=1}^{n_{\text{PRB}}} M_{u,k}(i) \tag{7}$$

where $sf(i) =$ NORMAL and n_{PRB} is the number of PRBs. And similarly in the small cell layer, where the average of the PF metrics is taken only during ABS:

$$PF^s(i) = \frac{1}{u_{\text{small}}} \sum_{u=1}^{u_{\text{small}}} \sum_{k=1}^{n_{\text{PRB}}} M_{u,k}(i) \tag{8}$$

where $sf(i) =$ MANDATORY or OPTIONAL.

The dynamics of the algorithm is as follows: The muting ratio β is adjusted depending on the PF metrics of the two layers. In contrast to IL-ABS, this algorithm works on an ABS periodic basis. The reason for that is that the algorithm

works with averaged metrics that are updated every T_{ABS}. At the begining of the ABS period it is decided if β is increased, decreased, or unchanged as compared to the last ABS period. Therefore, the maximum variation of β in one cycle is $1/T_{ABS}$. Particularly, more ABS resources will be assigned if the small cell layer is deteriorating (i.e. its average PF metrics is increasing) and at the same time the macro layer is improving (i.e. its average PF metrics is decreasing):

$$(PF^s(i) > PF^s(i-1)) \textbf{ and } (PF^m(i) < PF^m(i-1))$$

$$\textbf{and } (\beta < 1 - 1/T_{ABS}) \tag{9}$$

Naturally, β cannot be indefinitely increased, and the upper limit is imposed by the size of the ABS period and the fact that at least one normal subframe has to be set aside for measurement purposes. If (9) is not fulfilled, then it is checked if the macro cell is deteriorating:

$$(PF^m(i) > PF^m(i-1)) \textbf{ and } (\beta > 1/T_{ABS}) \tag{10}$$

Similarly as (9), β cannot be decreased if the minimum number of ABS, limited by the minimum number of mandatory ABS, has been reached. If none of the two conditions (9) and (10) is fulfilled, then β is kept at the same value as the last ABS period.

Analogously to IL-ABS, the algorithm ensures first of all the service of macro users, since the coverage area of the macro eNB is much larger, and the macro cell-edge users do not have the option of being scheduled with reduced interference conditions. The pseudo code for this algorithm can be found in Algorithm 2.

D. Fast ABS Adaptation in Distributed RRM Solutions

The fast ABS adaptation algorithms (IL-ABS and PF-ABS) are tailored to be applied for the centralized architecture (Scenario 3 in Figure 2), where all necessary information is available at the macro, including CQI for all UEs in the cluster, instantaneous load information for all cells in the cluster, and scheduling decision and related metrics (e.g. PF metrics as needed for the PF-ABS scheme). Essentially fast decisions in the centralized architecture are made shortly before each optional ABS on whether to configure as ABS or normal transmission. However, the fast IL-ABS and PF-ABS algorithms can also be decomposed to be applicable for the distributed architecture (Scenario 2). This is possible by having the macro acting as master for each cluster, in charge of fast ABS decisions based on information exchange with the small cells over the X2 interface. For the IL-ABS algorithm, the macro eNB needs to acquire knowledge of the number of RE users in all the small cells, whereas for the PF-ABS algorithm the averages of the PF metrics at the different small cells need to be collected.

The rate of fast ABS adaptation for the distributed architecture is therefore dependent on how frequent the aforementioned information is exchanged between cells in the cluster, as well as the X2 signaling delays. One option is to have the small cells periodically reporting the required information to the macro every N TTIs (subframes). Another option is that

---

Algorithm 2 Proportional Fair Based Algorithm (PF-ABS)

```
1:  i = 0
2:  while (i < i_max) do
3:     if  (PF^s(i) > PF^s(i-1))  and  (PF^m(i) <
        PF^m(i-1)) and (β < 1 - 1/T_ABS) then
4:        β = β + 1/T_ABS
5:     else
6:        if (PF^m(i) > PF^m(i-1)) and (β > 1/T_ABS) then
7:           β = β - 1/T_ABS
8:        end if
9:     end if
10:    update(PF^s)
11:    update(PF^m)
12:    i = i + 1
13: end while
```

---

the small cells inform the macro whenever a significant change in their load or PF metric is observed, i.e. event-triggered reporting. Notice that in any case the inter-eNB reporting is independent of the number of optional ABS per period, and there is no signal overhead at the air-interface from this solution. As an example, the upper part of Figure 5 shows a case where the IL-ABS algorithm is applied for the distributed architecture with periodic information exchange between small cells and macro. Every N TTIs the small cell informs the macro eNB of the number of users in critical interference conditions (RE users). Naturally, this information arrives at the macro with some intrinsic X2 delay. Based on that, the macro eNB can decide on the muting ratio to be applied, followed by informing the small cells how the macro will configure coming optional ABS. The period N is fixed and has to be designed for low load conditions in the network, when the average call duration is smaller and more frequent updates are needed for a proper performance. Similarly, an example of event-triggered updates is shown in the lower part of Figure 5, where the delay between the arrival/departure of the user and the available information in the macro eNB is illustrated. The amount of X2 signaling exchange is directly proportional to the arrival rate. In both cases (periodic or event-triggered) once the macro has decided how to configure the next optional ABS, it needs to inform the small cells, as they need this information for performing packet scheduling and link adaptation decisions in coherence with the experienced interference from the macro-layer.

V. PERFORMANCE ASSESSMENT

A. Simulation Methodology

In line with the system model outlined in Section II-A, the network topology consists of a standard hexagonal grid of three-sector macro eNBs complemented with a set of outdoor small cells. Macros and small cells share the same 10 MHz of bandwidth at a carrier frequency of 2 GHz. A directional 3D antenna pattern with down-tilt is modeled for the macro cells as defined in [21], while small cells are equipped with omni-directional antennas. One cluster is composed of one macro cell and four underlaying small cells. There is a total of 7 macro sites (21 macro cells) with wrap around to
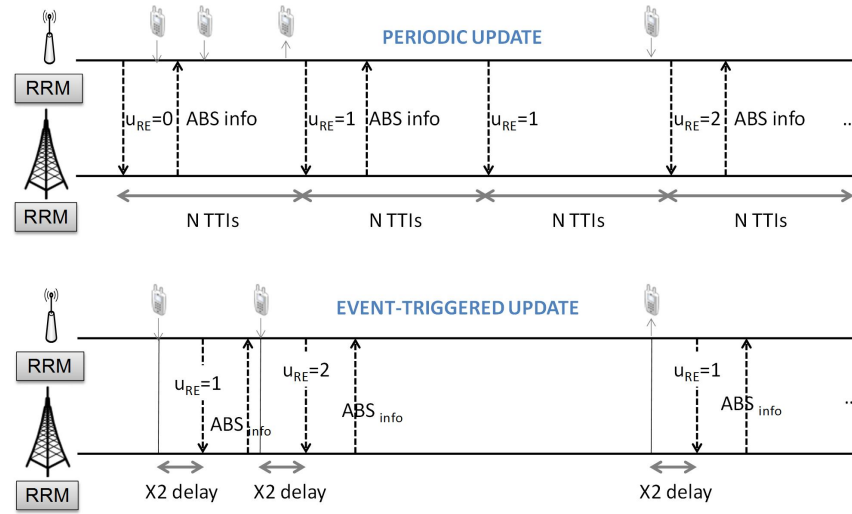
Fig. 5.   Example of fast ABS adaptation for distributed RRM solutions.

simulate the interference effect of a larger network. The macro intersite distance is 500 m, and the minimum distance among small cells is 40 m. The propagation model consists of a deterministic distance dependent component, as well as two independent stochastic components for shadow fading and fast fading. Shadow fading is modeled according to Gudmundson's model [28] [29], while the frequency selective fast fading is according to the Typical Urban model. The path loss exponent and shadow fading standard deviation is different for macro and small cell radio links, in line with the HetNet simulation assumptions in [21].

The simulator follows the LTE specifications, including detailed modeling of major RRM functionalities [30]. The same simulation methodology as outlined in [31] is adopted in coherence with the 3GPP simulation guidelines, where the time-resolution is one subframe. For each subframe, the experienced SINR for each scheduled user is calculated per subcarrier, assuming an interference rejection combining (IRC) receiver [32]. Given the SINR per subcarrier, the effective exponential SINR model [33] for link-to-system-level mapping is applied to determine if the transmission was successfully decoded. Failed transmissions are retransmitted using hybrid ARQ with ideal Chase Combining (CC) [34]. For the latter case, the effect of hybrid ARQ with CC is captured by the link-to-system model by linearly adding the SINRs for the different hybrid ARQ transmissions. The modulation and coding scheme for first transmissions is determined by the link adaption functionality based on frequency selective CQI measurement feedback from the UEs [30]. The small cell users are configured to report separated CQIs when the macro is using Normal and Mandatory ABS, as explained in Section III-B. Closed loop 2x2 single user MIMO with pre-coding and rank adaptation is assumed for each link [25]. Ideal cancellation of CRS interference during protected subframes (advanced users) is further assumed for the small cell users [26]. Users are scheduled according to the PF algorithm, as described in Section III-C. Management and prioritization of

scheduling new transmissions and hybrid ARQ retransmissions is according to [35]. The time-variant traffic model outlined in Section II-B is applied, assuming a payload size of $B = 1$ Mbit for each call. By default, a hotspot deployment model (the so-called model 4b in [21]) is assumed, with 2/3 of the users located in the vicinity of the small cells. In order to obtain statistical reliable results for the end-user throughput, simulations are run for a time-duration corresponding to at least 5000 completed calls. This is sufficient to have a reasonable confidence level for the considered KPIs. The default assumptions for the simulations are summarized in Table I.

B. Slow vs. Fast Muting Adaptation

Figures 6 and 7 show the 5%-ile and 50%-ile user throughput as a function of the average offered load $\bar{L}$. There are four curves, corresponding to no eICIC, slow muting adaptation (Scenario 1), and fast muting adaptation with IL-ABS and PF-ABS (Scenario 3). As expected, both the 5%-ile and the 50%-ile user throughput decrease as $\bar{L}$ increases for all cases.

For slow muting adaptation, the optimal eICIC parameter settings for the different values of average offered load are indicated (aiming at maximizing the 5%-ile throughput) [16]. Both β and RE are adjusted to track the average envelope of the offered traffic, with β varying from 0% to 100% muting and RE from 0 dB to 20 dB. It is illustrated how the optimal eICIC configuration varies versus the offered traffic load by displaying the best settings of β and RE (found by extensive simulation search). At low offered load, there is little, or marginal, gain from applying eICIC. This is due to the fact that there is only marginal other-cell interference, and the gain in this low loaded cases comes from the application of a small RE offset at the pico. As the offered load increases, both macros and picos start having higher probability of transmitting (and thus causing interference to other cells), and the system converges to using more ABS at the macros and higher RE at the picos.

TABLE I.   SUMMARY OF DEFAULT SIMULATION ASSUMPTIONS

Network Layout	500 m macro-layer Inter-Site Distance with 4 small eNBs per macro cell
Cell layout	7 macro sites (21 macro cells), wrap-around
Transmit power	macro eNB: 46 dBm; small eNB: 30 dBm
Bandwith	10 MHz at 2 GHz carrier frequency
Subframe duration	1 ms (11 data plus 3 control symbols)
Modulation and coding schemes	QPSK (1/5 to 3/4), 16-QAM (2/5 to 5/6), 64-QAM (3/5 to 9/10)
HARQ modeling	Ideal chase combining with maximum 4 transmissions, 10% block error rate target
Transmission mode	2x2 closed loop with rank adaptation
Antenna gain	Macro: 14 dBi; small cell: 5 dBi; UE: 0 dBi
Antenna pattern	Macro: 3D [21]; small cell and UE: omni directional
Macro path loss	128.1 [dB]+37.6 [dB]$\cdot \log_{10}(R[km])$, where R is the macro eNB to UE distance
Small cell path loss	140.7 [dB]+36.7 [dB]$\cdot \log_{10}(R[km])$, where R is the small cell eNB to UE distance
Shadow fading	Lognormal, std = 10 dB for small eNB to UE links, 8 dB for macro eNB to UE links
eNB packet scheduler	Proportional Fair (PF)
UE capabilities	Interference Rejection Combining; UEs with ideal CRS IC
Simulation Time	[10..25] seconds

With fast muting adaptation, the RE is assumed to be adjusted in coherence with the average offered load by means of a load balancing optimization algorithm [7] (the optimal value in the Figures found by simulation search), while β is dynamically adjusted by the algorithm. One could think there is a tradeoff between the number of semi-static subframes and the number of optional subframes: decreasing the number of normal and mandatory ABS increases the dynamicity of the fast adaptation, but at the same time it reduces the reliability of the reported CQI, that has less chances to get a proper estimation of the pilot signals. However, as it is observed here, the loss in accuracy of the CQI is by far compensated by the gains of the flexible adaptation, such that the best configuration is to reduce the number of normal and mandatory ABS to the minimum (1 subframe), even with realistic modeling of the link adaptation procedures. Thus, β can vary from 1/8 to 7/8 ($T_{ABS} = 8$). Regarding the RE, the behaviour is analogous to the slow ABS muting adaptation: For low load, small values of RE are recommended because of the low number of users in the system. As the load increases, it is convenient to offload users to the small cell layer by application of higher values of the RE offset. However, the optimal RE when using dynamic ABS is lower than the slow case, due to the better load balancing from using the appropriate ABS at each time.

The gain of eICIC compared to no eICIC is well-known [5] - [6]. In Figures 6 and 7 it is observed that there is still a significant gain both in 5%-ile and 50%-ile when moving from slow muting adaptation to faster dynamic solutions, for both algorithms, with PF-ABS outperforming IL-ABS. The reason for the latter is that PF-ABS is capturing the channel condition by means of the average PF metric of the macro and the small cell layer, whereas IL-ABS is mainly focused on the load conditions. For a target 5%-ile outage throughput of 2 Mbps, the slow adaptation supports ∼33 Mbps of offered load, while the IL-ABS algorithm allows up to ∼50 Mbps and PF-ABS up to ∼52 Mbps, leading to a relative gain of ∼40%. Similarly, the relative gains for a capacity of 3 Mbps and 5 Mbps are in the order of 40-60%. The results correspond to a payload of $B =$1 Mbit per call, but higher values of payload (up to 10 Mbits) have been also simulated. Not only the trends and conclusions discussed here remain the same, but also the relative gains are in the same range.

Another important factor is the user distribution. In the results we assume a hotzone distribution, where 2/3 of the users are within the hotspot area and the remaining 1/3 is uniformly distributed in the macro coverage area. Simulations with spatial uniform distribution of the users have been also run. Naturally, the throughput using eICIC is lower as compared to having a hotspot distribution, with a good percentage of users concentrated around the small cells. However, the relative gain of having fast decisions as compared to slow ABS adaptation remains in the range of 40-60%.

In Figure 8 the CDF of the muting ratio β of one of the macro cells is plotted for different values of call arrival rate and for IL-ABS and PF-ABS. For comparison, also the optimal semi-static muting ratio in Scenario 1 is indicated with circles for the different arrival rates. In both algorithms the key aspect is the application of the minimum β (1/8) most of the time: When $\bar{L}$ is low, both the macro and the small cell layer are empty most of the time, and the algorithm tends to use the smallest muting ratio. As the user arrival rate increases, the differences between layers become noticeable. In both cases the probability of empty cell decreases, and the number of active users increases, but the growth is much more significant in the macro layer. Thus, it is straightforward that IL-ABS will try to serve first the macro layer (due to the higher instantaneous macro load), using again the minimum muting ratio most of the time. In the case of PF-ABS, the number of macro users increases, and so does the average PF metric of the layer, and hence the algorithm reduces β.

C. Fairness

Figure 9 shows the Jains fairness index as a function of $\bar{L}$, for slow and fast muting adaptation with IL-ABS and PF-ABS. It is observed how the index decreases with the offered load, but the degradation is much more significant for the slow muting adaptation, not able to capture the instantaneous load and channel variations. Moreover, PF-ABS provides more fairness to the users as compared to IL-ABS, thanks to the inclusion of the instantaneous channel condition in the decision.

D. Centralized vs. Distributed RRM

Finally, we study the performance of the fast adaptation in distributed architectures, by exploiting enhanced information
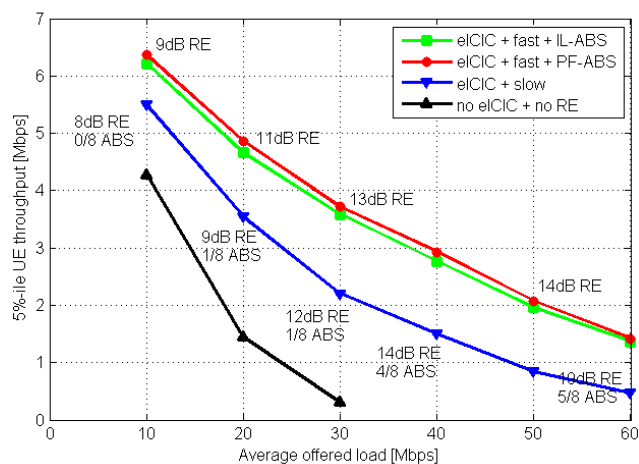
Fig. 6.   5%-ile user throughput as a function of the average offered load with no eICIC, eICIC with slow muting adaptation and eICIC with fast muting adaptation.
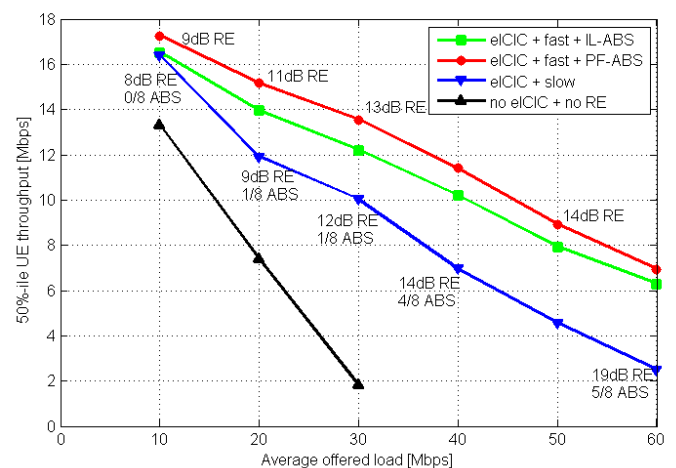

Fig. 7.   50%-ile user throughput as a function of the average offered load with no eICIC, eICIC with slow muting adaptation and eICIC with fast muting adaptation.

exchange over X2, as compared to the centralized architecture (upper bound) and the slow or semi-static adaptation (lower bound). By doing so, we can in practice benefit from the good gains of the fast adaptation with very little effort, by enhancing the current signaling in the 3GPP standard.

1) Periodic Updates: Figure 10 shows the performance of the IL-ABS algorithm in Scenario 2, in which the required information is updated periodically every N subframes, where N ranges from 80 to 320 TTIs. If N is smaller than the average call duration, then the results are fairly close to the centralized solution. Moreover, for very short calls the number of users fluctuates rapidly, and even the shortest period of 80 TTIs is not enough to track the traffic fluctuations. It has been observed in simulations that the average call duration for 10 Mbps of offered load is approximately 75 TTIs, while for 60 Mbps it goes up to 250 TTIs. For comparison purposes we show with thick and solid line two thresholds: with very slow updates, the performance gets closer to the slow adaptation (scenario 1), while when the period is short enough, the throughput approaches the performance of the centralized solution (Sscenario 3). On the other hand, as the load increases, the arrival and departure of users (RE or macro) in a period is less significant as compared to the total number of users, and hence the performance of the distributed solution approaches the centralized case indepedently of the update period. Notice that the simulations have been run with a low value of payload of 1 Mbit, leading to significant traffic fluctuations in the system (worst case for our purposes). With a higher value of payload, smaller differences between the distributed and the centralized RRM scenario are observed. Even though not shown, it has been observed that with $B = 10$ Mbits of payload the cell-edge and median user throughputs get very close to the centralized case even with $N = 320$ TTIs (i.e. with little signaling exchange effort).

2) Event-triggered Updates: Figure 11 plots the 5%-ile user throughput of IL-ABS algorithm in Scenario 2 with event-

triggered information updates, i.e. the small cell informs the macro everytime a small cell user arrives to or leaves the network. Moreover, this information arrives at the macro layer after some delay, that has been set to 5 and 50 ms. We can see that with 5 ms of delay, a commonly assumed value, the 5%-ile user throughput is quite close to the upper bound, with relative losses in the order of 5-8%. As the delay increases, the fast adaptation is not able to track the rapid traffic fluctuations and the performance degrades.

VI.   CONCLUSIONS

A simple eICIC framework for fast ABS adaptation in HetNets with macro cells and small cells is developed, aiming at boosting the network performance by means of dynamic muting decisions. The fast muting adaptation can be applied not only to centralized RRM solutions, but also to distributed RRM architectures, where enhanced information exchange over X2 interface is exploited. We propose two different algorithms that adjust the ABS muting dynamically according to the instantaneous load conditions (IL-ABS) and the average PF metrics (PF-ABS), respectively. The input required by the algorithms reduces to the number of macro users and the number of small cell users in the worst interference conditions, and the average PF metrics in both layers. Performance results for the centralized RRM architecture with RRHs show capacity gains of 40-50% for fast adaptation in scenarios with bursty traffic (both low and high load) as compared to cases with semi-static ABS patterns that can only be adjusted on time-scales of several seconds. The fast muting adaptation also improves significantly the fairness among users, especially noticeable at high offered load. The PF-ABS algorithm slightly outperforms IL-ABS not only in performance, but also in fairness, thanks to its ability to capture the user channel condition by means of the proportional fair metric. Finally, it is shown that we can achieve comparable performance in the
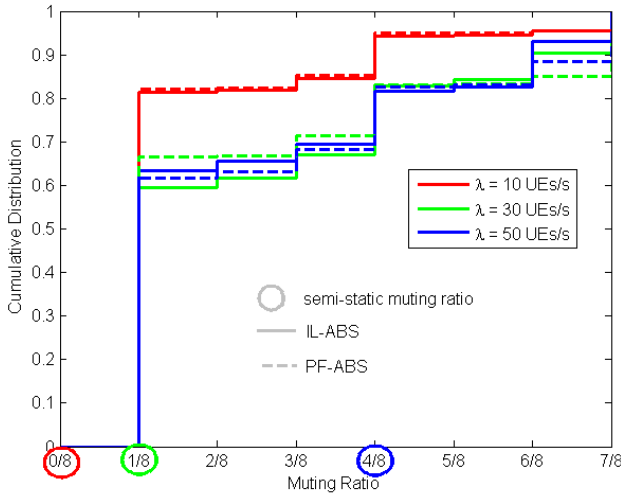
Fig. 8. CDF of the muting ratio β for slow adaptation and fast adaptation with IL-ABS and PF-ABS.

Fig. 9. Jain's fairness index as a function of the average offered load and for slow adaptation and fast adaptation with IL-ABS and PF-ABS.

distributed RRM architecture with picos and in the centralized architecture with RRHs, provided that the inter-node signaling latency is lower than the typical time of significant traffic fluctuations in the network. As an example, nearly identical performance is observed for centralized architecture with RRH and distributed solutions with picos for cases where the X2 latency is 5 ms, despite the rapid fluctuations in the number of schedulable users of the considered traffic model.

ACKNOWLEDGMENT

REFERENCES

[1] A. Khandekar, N. Bhushan, J. Tingfang, and V. Vanghi, "LTE-Advanced: Heterogeneous Networks, " *IEEE European Wireless Conference*, pp. 978 -982, April 2010.

[2] A. Damnjanonic, J. Montojo, Y. Wei, J. Tingfang, T. Luo, M. Vajapeyam, T. Yoo, O. Song, D. Malladi, "A Survey on 3GPP Heterogeneous Networks, " *IEEE Wireless Communications Magazine*, vol. 18, no. 3, pp. 10-21, June 2011.

[3] A. Ghosh, R. Ratasuk, B. Mondal, N. Mangalvedhe, and T. Thomas, "LTE-Advanced: next-generation wireless broadband technology, " *IEEE Wireless Communications*, vol. 17, no. 3, pp. 10-22, June 2010.

[4] P. Bhat, S. Nagata, L. Campoy, I. Berberana, T. Derham, G. Liu, X. Shen, P. Zong, and J. Yang, "LTE-Advanced: An Operator Perspective," *IEEE Wireless Communications Magazine*, vol. 50, no. 2, pp. 104-114, Feb. 2012.

[5] B. Soret, H. Wang, K.I. Pedersen, and C. Rosa, "Multicell Cooperation for LTE-Advanced Heterogeneous Network Scenarios," *IEEE Wireless Communications Magazine*, vol. 20, no. 1, pp. 27-34, Feb. 2013.

[6] D. López-Pérez, X. Chu, and I. Güvenç, "On the Expanded Region of Picocells in Heterogeneous Networks," *IEEE Journal of Selected Topics in Signal Processing*, vol. 6, no. 3, pp. 281-294, June 2012.
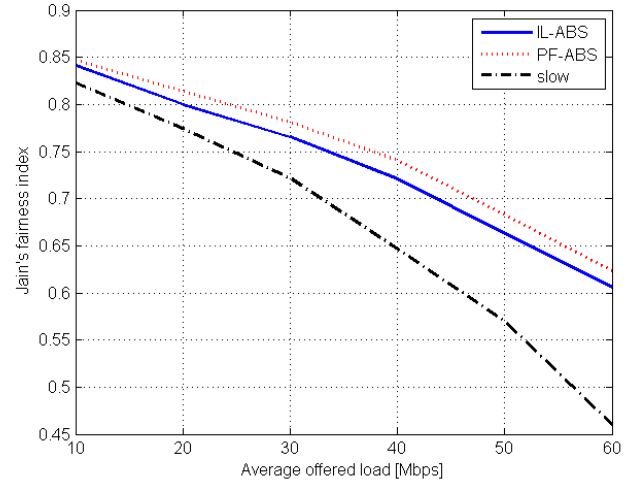
[7] S. Hämäläinen, H. Sanneck, and C. Sartori, "LTE Self-Organizing Networks (SON): Network Management Automation for Operational Efficiency," *J. Wiley & Sons*, United Kingdom, 2012.

[8] P. Muñoz, R. Barco, and I. de la Bandera, "On the Potential of Handover Parameter Optimization for Self-Organizing Networks," *IEEE Transactions on Vehicular Technology*, vol. 62, no. 5, pp. 1895-1905, June 2013.

[9] Q. Ye, B. Rong, Y. Chen, C. Caramanis, and J. Andrews, "Towards an Optimal User Association in Heterogeneous Cellular Networks," *IEEE Global Communications Conference (GLOBECOM)* , pp. 4143-4147, Dec. 2012.

[10] J. Pang, J. Wang, D. Wang, G. Shen, Q. Jiang, J. Liu, "Optimized Time-Domain Resource Partitioning for Enhanced Inter-Cell Interference Coordination in Heterogeneous Networks," *IEEE Wireless Communications and Networking Conference (WCNC)*, pp. 1613-1617, April 2012.

[11] A. Bedekar, and R. Agrawal, "Optimal Muting and Load Balancing for eICIC," *International Symposium and Workshops on Modeling and Optimization in Mobile, Ad Hoc and Wireless Networks (WiOpt)*, pp., 280-287, May 2013.

[12] B. Soret, and K.I. Pedersen, "Macro Cell Muting Coordination for Non-Uniform Topologies in LTE-A HetNets," *IEEE Vehicular Technology Conference (VTC) Fall 2013*, Sept. 2013.

[13] C. Qvarfordt, and P. Legg, "Evaluation of LTE HetNet deployments with realistic traffic models," *IEEE 17th International Workshop on Computer Aided Modeling and Design of Communication Links and Networks (CAMAD)*, pp. 307-311, Sept. 2012.

[14] Y.N. Ruyue, J. Li, W. Li, Y. Xue, and H. Wu, "CoMP and Interference Coordination in Heterogeneous Network for LTE-Advanced," *IEEE Global Communications Conference (GLOBECOM)*, pp. 1107-1111, Dec. 2012.

[15] Y. Wang, X. She, and L. Chen, "Enhanced Dynamic Inter-Cell Interference Coordination Schemes for LTE-Advanced," *IEEE Vehicular Technology Conference (VTC)*, Sept. 2012.

[16] K.I. Pedersen, Y. Wang, B. Soret, and F. Frederiksen, "eICIC Functionality and Performance for LTE HetNet Co-Channel Deployments," *IEEE Vehicular Technology Conference (VTC) Fall 2012*, Sept. 2012.

[17] Y. Wang, and K.I. Pedersen, "Time and Power Domain Interference Management for LTE Networks with Macro-cells and HeNBs, " *Proceedings IEEE Vehicular Technology Conference (VTC) Fall 2011*, Sept. 2011.
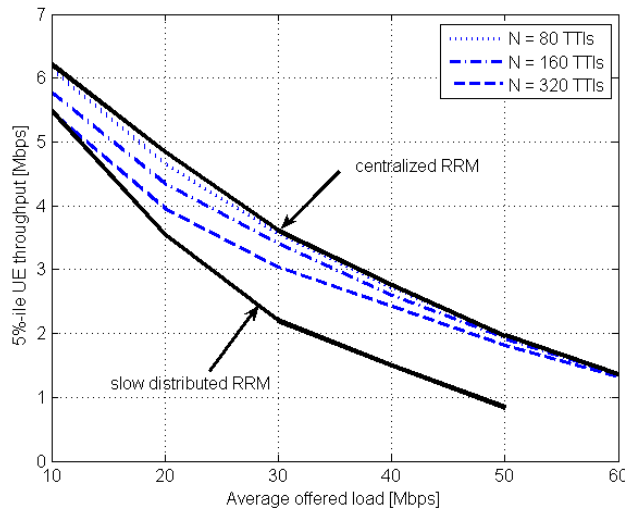
Fig. 10.   5%-ile user throughput with fast distributed RRM solutions based on X2. Periodic updates.
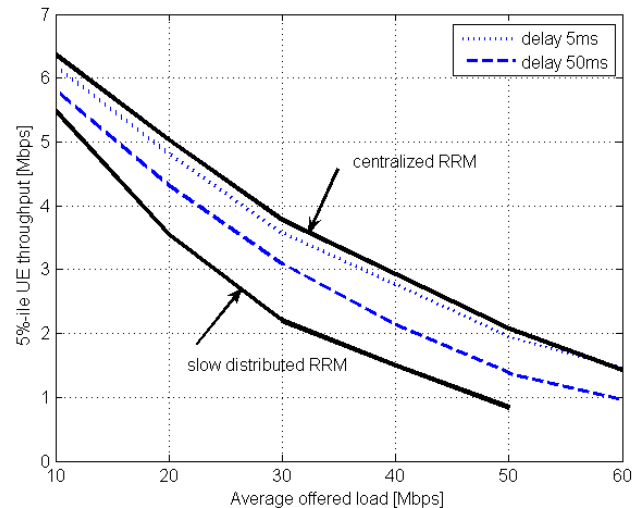

Fig. 11.   5%-ile user throughput with fast distributed RRM solutions based on X2. Event-triggered updates.,

[18] K.I. Pedersen, T. E. Kolding, F. Frederiksen, I. Z. Kovács, D. Laselva, and P. E. Mogensen, "An Overview of Downlink Radio Resource Management for UTRAN Long-Term Evolution," *IEEE Communications Magazine*, vol. 47, no. 7, pp. 86-93, July 2009.

[19] B. Soret, K.I. Pedersen, T.E. Kolding, H. Kroener, and I. Maniatis, "Fast Muting Resource Allocation for LTE-A HetNets with Remote Radio Heads," *Proceedings IEEE Global Communications Conference (GLOBECOM) 2013*.

[20] A. Tukmanov, Z. Ding, S. Boussakta, and A. Jamalipour, "On the Impact of Network Geometric Models on Multicell Cooperative Communication Systems," *IEEE Wireless Communications Magazine*, vol. 20, no. 1, pp. 75-81, Feb. 2013.

[21] 3GPP Technical Report 36.814, "Further Advancements for E-UTRA Physical Layer Aspects," version 9.0.0, March 2010.

[22] A. Damnjanovic, J. Montojo, J. Cho, H. Ji, J. Yang, and P. Zong, "UE's Role in LTE Advanced Heterogeneous Networks," *IEEE Communications Magazine*, vol. 50, no. 2, pp. 164-176, Feb. 2012.

[23] P. Ameigeiras, Y. Wang, J. Navarro-Ortiz, P. E. Mogensen, and J. M. Lopez-Soler, "Traffic Models Impact on OFDMA Scheduling Design," *EURASIP Journal on Wireless Communications and Networking*, doi:10.1186/1687-1499-2012-61, Feb. 2012.

[24] R. Jain, D. Chiu, and W. Hawe, "A quantitative measure of fairness and discrimination for resource allocation in shared systems," *tech. rep. Digital Equipment Corporation, DEC-TR-301*, Sept. 1984.

[25] S. Sesia, I. Toufik, and M. Baker, "LTE - The UMTS Long Term Evolution: From Theory to Practice," *John Wiley & Sons Ltd.*, Great Britain, 2009.

[26] B. Soret, Y. Wang, and K.I. Pedersen, "CRS Interference Cancellation in Heterogeneous Networks for LTE-Advanced Downlink ," *IEEE International Conference on Communications ICC 2012 (International Workshop on Small Cell Wireless Networks)*, pp. 6797-6801, June 2012.

[27] F. Kelly, "Charging and Rate Control for Elastic Traffic," *European Transactions on Telecommunications*, vol. 8, pp. 33-37, Jan. 1997.

[28] M. Gudmundson, "Correlation model for shadow fading in mobile radio systems," *IEEE Electronic Letters*, vol. 27, no. 23, pp. 2145-2146, Nov. 1991.

[29] S. S. Szyszkowicz, H. Yanikomeroglu, and J. S. Thompson, "On the Feasibility of Wireless Shadowing Correlation Models, *IEEE Trans-*

actions on Vehicular Technology, vol. 59, no. 9, pp. 4222-4236, Nov. 2010.

[30] K.I. Pedersen, T.E. Kolding, I.Z. Kovács, G. Monghal, F. Frederiksen, and P.E. Mogensen, "Performance Analysis of Simple Channel Feedback Schemes for a Practical OFDMA System, " *IEEE Transactions on Vehicular Technology*, vol 58, no. 9, pp. 5309-5314, Nov. 2009.

[31] M. Rinna, M. Kuusela, and E. Tuomaala, P. Kinnunen, I.Z. Kovács, K. Pajukoski, and J. Ojala, "A Performance Summary of the Evolved 3G (E-UTRA) for Voice Over Internet and Best Effort Traffic, " *IEEE Transactions On Vehicular Technology*, vol. 58, no. 7, pp. 3661-3673, Sept. 2009.

[32] J. Winters, "Optimum combining in digital mobile radio with cochannel interference," *IEEE Journal on Selected Areas in Communications*, vol. 2, no. 4, pp. 528-539, July 1984.

[33] K. Brueninghaus, D. Astely, T. Salzer, S. Visuri, A. Alexiou, S. Karger, and G.A. Seraji, "Link performance models for system level simulations of broadband radio access systems," *IEEE Personal, Indoor and Mobile Radio Communications (PIMRC)*, pp. 2306-2311, Sept. 2005.

[34] D. Chase, "Code combining: A maximum-likelihood decoding approach for combining an arbitrary number of noisy packets," *IEEE Transactions on Communications*, vol. 33, no. 5, pp. 385-393, May 1985.

[35] A. Pokhariyal, K. I. Pedersen, G. Monghal, I.Z. Kovács, C. Rosa, T.E. Kolding, and P.E. Mogensen, "HARQ aware frequency domain packet scheduler with different degrees of fairness for the UTRAN long term evolution," *IEEE Vehicular Technology Conference Spring 2007*, pp. 2761-2765, Apr. 2007.

Beatriz Soret received her M.Sc. and Ph.D. degrees in telecommunication engineer from the University of Mlaga, Spain, in 2002 and 2010, respectively. She is currently a Radio Research Specialist at Nokia Solutions and Networks. Before, she was an assistant professor at Malaga University in 2006-2011 and a postdoc at Aalborg University in 2011-2013. Her current research work is focused on heterogeneous networks and radio resource management for 4G cellular systems and 3GPP standardization of LTE. She received the best paper award in IEEE Globecom 2013.

Klaus I. Pedersen received his M.Sc. E.E. and Ph.D. degrees in 1996 and 2000 from Aalborg University, Denmark. He is currently with Nokia Solutions and Networks in Aalborg, where he is a senior wireless network specialist. His current work is related to radio resource management and 3GPP standardization of LTE, and its future evolution. The latter includes work on heterogeneous networks, mobility, interference management, and system performance assessment. He is the author/co-author of more than hundred peer reviewed publications on a wide range topics, as well as an inventor on several patents. Finally, he is appointed as part-time professor at Aalborg University in the radio access technology section.